

COMPLEX STRUCTURE IN RXJ1347.5-1145: MAJOR MERGER OR ONE OF THE MOST ENERGETIC AGN OUTBURSTS KNOWN?

1 Structure in the Core of RXJ1347.5-1145

RXJ1347.51145 ($z = 0.451$) is one of the most X-ray luminous and massive galaxy cluster known. It has been extensively studied in the X-ray (Allen et al., 2002; Gitti & Schindler, 2004; Miranda et al., 2008) and has historically been considered a massive cooling flow cluster. It has also been the subject of a number of studies to measure the Sunyaev-Zeldovitch effect (SZE) (Pointecouteau et al., 1999, 2001; Komatsu et al., 2001; Kitayama et al., 2004). These studies have identified a region of enhanced surface brightness and high temperature widely interpreted as evidence for an ongoing merger. However a number of lensing studies would seem to contradict the simple merger explanation for the observed X-ray structure in RXJ1347.5-1145 (Halkola et al., 2008; Lu et al., 2010). In addition, recent MUSTANG bolometer data show a complex SZE morphology that implies a more complicated origin for the observed SZE excess (Mason et al., 2009).

Our analysis of the existing *Chandra* observations has revealed tentative evidence for a pair of cavities straddling the nucleus of the BCG. Cavity systems like these have been identified in more than two dozen clusters, and are generally associated with radio jets in powerful AGN (Bîrzan et al., 2004). Comparison between the X-ray images and recent MUSTANG bolometer SZE maps show a rough correlation between the apparent cavities and the observed excess SZE signal. This result is potentially important for several reasons. First, the suggestion that the enhanced SZE signal is due to shock heated gas by a merger is weakened. It is unclear how a symmetric cavity system would be created during a merger, and it is even less likely that the enhanced SZE signal in RXJ1347-1145 would be randomly associated with the cavities.

We suggest instead that the SZE enhancement, which traces the integral of thermal pressure along the line of sight, is due to a hot thermal plasma that is pressurizing the expanding AGN cavities. This interpretation has a number of important implications for studies of cavity energetics. It would imply that the relativistic $\gamma = 4/3$ radio plasma is not the dominant source of pressure. If instead, a hot, $\gamma = 5/3$ thermal gas provides the pressure, the total energy for the cavities would then be $E = 2.5pV$ rather than $4pV$ as is commonly assumed. If confirmed, it would be the first such detection and the only measurement of the state of the gas inside a radio cavity.

2 Evidence for X-ray Cavities in RXJ1347.5-1145

A slightly smoothed ($2''$ Gaussian) image of the central region of RXJ1347.5-1145 is shown in the upper left panel of Figure 1. As has been noted in the literature, the overall emission is fairly smooth and circular indicative of a relaxed, undisturbed cluster. The surface brightness enhancement to the SE however has been studied extensively in previous X-ray analyses (Schindler et al., 1997; Allen et al., 2002; Gitti & Schindler, 2004; Miranda et al., 2008) and has been interpreted as evidence that the cluster is undergoing a major merger event. The image also exhibits surface brightness discontinuities to the E and W sides of the bulk of the cluster emission. These features are reminiscent of the discontinuities associated with cavity systems in many other X-ray clusters. These structures are more readily apparent in the unsharp-masked image shown in the upper right panel of Figure 1. The image was created by dividing images smoothed with $2''$ and $10''$ Gaussians.

The resulting depressions in the surface brightness are statistically significant ($> 4\sigma$) relative to the smooth background profile and resemble similar structures seen in many other cavity systems. Interpreting evidence for cavities based on X-ray data alone is difficult given the complicated structures routinely found in cluster cores with *Chandra* imaging. Traditionally, the presence of

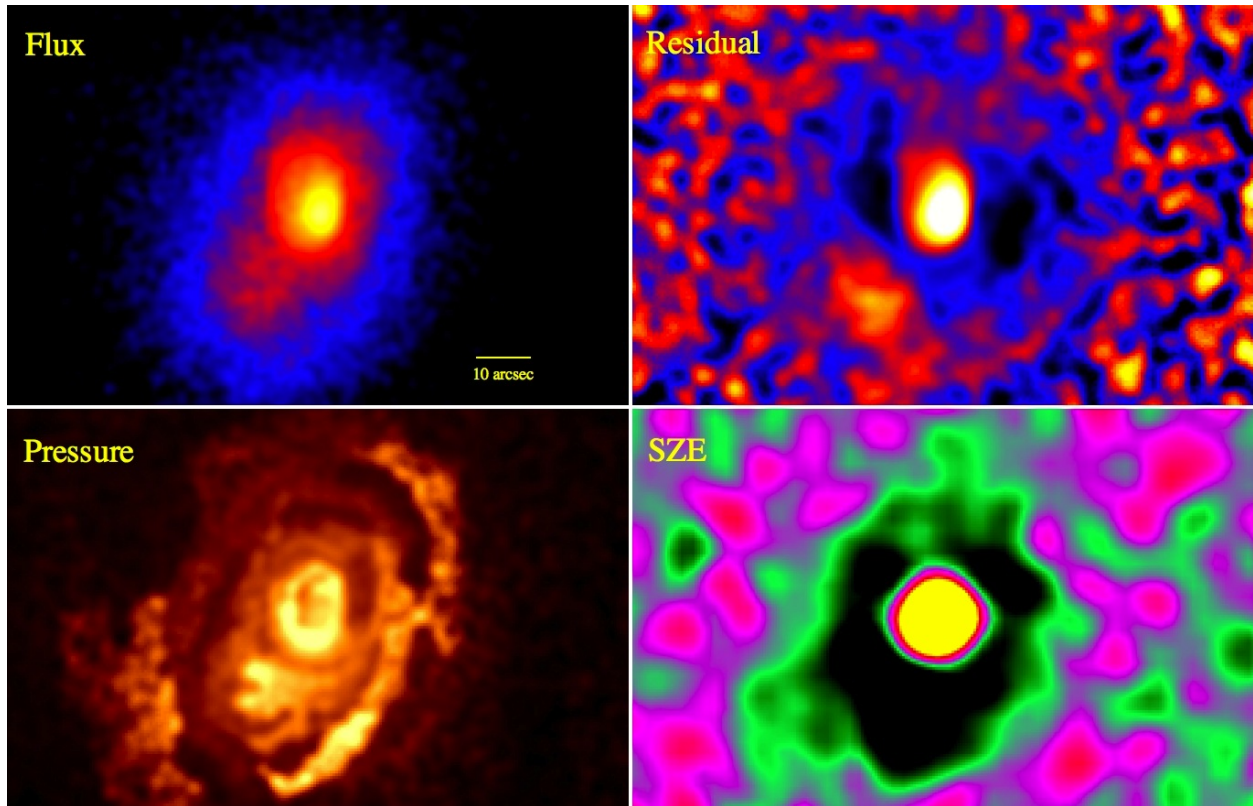


Figure 1: **UL:** An image made from 63 ksec of archival *Chandra* data on RXJ1347.5-1145, the most luminous X-ray cluster known. The horizontal yellow bar indicates a spatial scale of 10 arcsec (58 kpc). **UR:** Unsharp masked image of the core of RXJ1347.5-1145 showing evidence for a possible cavity system. **LL:** Pressure map of RXJ1347.5-1145 based on the derived temperature map. **LR:** An image of the SZE in RXJ1347-1145 taken with the MUSTANG bolometer array on the Green Bank Telescope (GBT) (Mason et al., 2009). The noise in the map is ~ 0.3 mJy/beam. The spatial scale is the same in all images.

high or low frequency radio emission filling the cavities has been used as circumstantial evidence that the cavity structures were both real and associated with the central AGN (Bîrzan et al., 2004). Unfortunately the available radio data for RXJ1347.5-1145 is somewhat poor. Gitti et al. (2007) have presented 1.4 GHz VLA images (A configuration) of RXJ1347.5-1145 with a resolution of $1.7'' \times 1.2''$. The central radio source is resolved and exhibits a total flux density of 29.8 mJy. The radio image shows evidence for faint structures (detected at the 6σ level) emanating to the E and NW directions from the center in the direction of the observed X-ray depressions. Although perhaps suggestive, these results are far from conclusive. Deeper radio data will ultimately be necessary to verify if the radio-X-ray anti-correlation observed in other clusters holds for RXJ1347.5-1145.

The map of the measured Sunyaev-Zeldovich effect (SZE) in RXJ1347.5-1145 shown in the lower right panel of Figure 1 however suggests an intriguing possibility. This image was taken with the MUSTANG bolometer array on the Green Bank Telescope (GBT) and has a $10''$ resolution (Mason et al., 2009). The intensity of the SZE map peaks in the vicinity of the SE surface brightness enhancement consistent with the interpretation that it is a large substructure of gas shock-heated ($T > 20$ keV) by a major merger. Interestingly, strong SZE values of almost equal intensity are also found at the corresponding locations of the possible cavity structures to the E and W of the cluster center. This correlation suggests the possibility that, if real, the cavities in RXJ1347.5-1145 are filled with a very, hot thermal plasma ($T \sim 25$ keV) rather than relativistic plasma as seems to

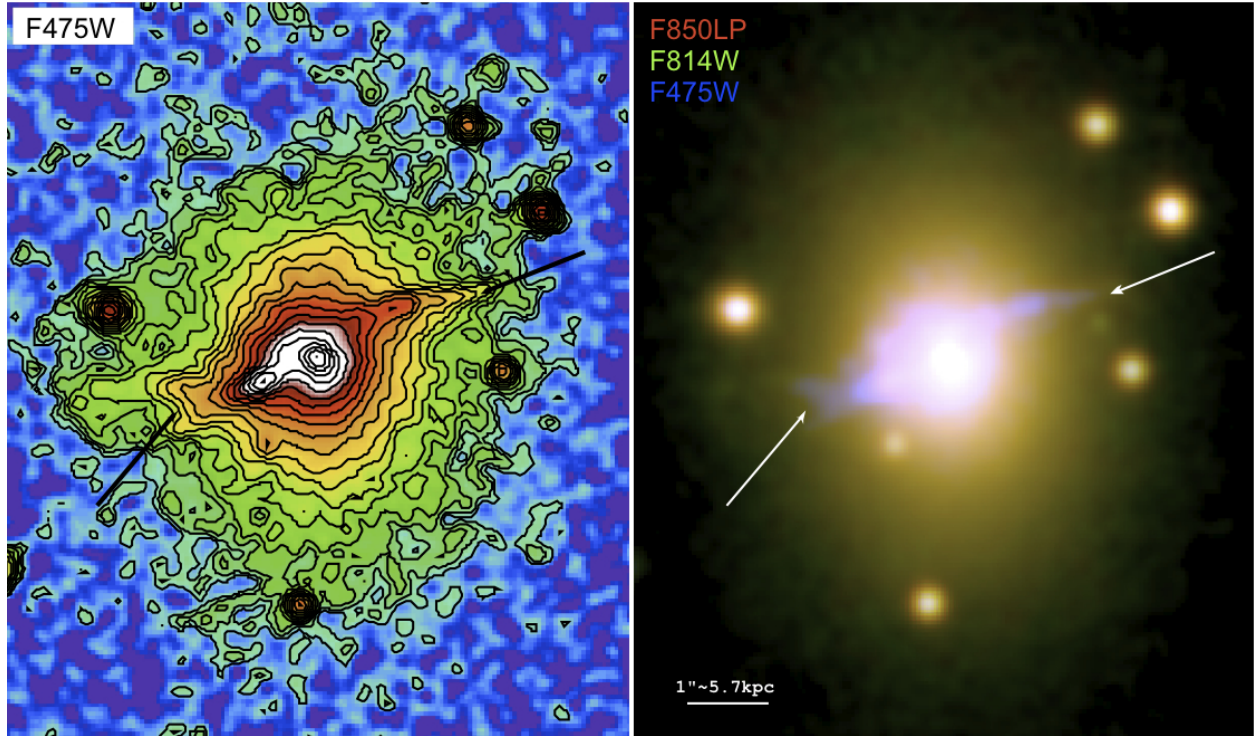


Figure 2: **Left:** This figure shows images created from the Hubble Legacy Archive data of the BCG in RXJ1347.5-1145. **Left:** The F475W band image of the core of RXJ1347.5-1145 with the contours of the isophotes overlaid. The extensions to the east and northwest are easily visible. **Right:** A composite image constructed from the F475W, F814W, and F850LP filter images. The blue jet-like structure is clearly visible.

be the case in many other cavity systems. The high temperature and thermal origin of the emission in RXJ1345.5-1145 have been confirmed by recent *Suzaku* observations (Ota et al., 2008). What fills the interiors of observed X-ray cavities is an open question in the study of these systems.

Further evidence supporting the cavity interpretation can be seen in the archival HST images for RXJ1347.5-1145 shown in Figure 2. These images show clear evidence for jet-like structures extending roughly ~ 2 -3 arcsec E and W from the center of the BCG. The endpoints of these extensions correspond spatially almost exactly with the sharp surface brightness discontinuities and inner edges of the cavity-like depressions seen in the X-ray data. Although circumstantial, the presence of such structures when combined with the X-ray and SZE data makes for a consistent picture of an AGN-induced cavity system in RXJ1347.5-1145.

If the observed cavity structures are associated with an AGN outburst, they represent an enormous amount of energy input into the ICM. Using the archival *Chandra* data for RXJ1347.5-1145, we have estimated the work required to inflate the observed cavities against the pressure of the surrounding ICM. Approximating the structures in Figure 1 as elliptical cavities roughly $4'' \times 8''$, we obtain a total energy to create both cavities of $3 - 6 \times 10^{60}$ ergs under the usual assumption that the cavities are filled with $\gamma = 4/3$ gas. With the temperature and density profile in the cluster, we can estimate ages for the cavity assuming typical sound speed arguments. The resulting cavity ages are 30-40 Myr. Combining these quantities yields an estimate for the mean energy output of the AGN of $2 - 6 \times 10^{46}$ ergs/s. If confirmed, these cavities therefore represent one of the most energetic systems known comparable to other giant outbursts such as Hercules A or MS0735.6+7421.

3 Specific Scientific Objectives

Our primary objective is to construct a detailed 2D spectral map of the core in RXJ1347.5-1145 and quantify the relative energy input into the ICM whether from mergers, shocks, or possible AGN outbursts. Be it shocks associated with a merger event or an AGN outburst, these observations will provide quantitative constraints on the amount and location of the deposited energy and by extension the physical processes driving that deposition. In addition, the requested deep exposure of such a well-studied object as RXJ1347.5-1145 will allow a wealth of ancillary science including mass and lensing studies. We briefly summarize our overall science goals here:

- **Physical State of the Plasma filling the Cavities:** A long-standing open question in the study of X-ray cavity systems is what is filling the cavities? The observed spatial correlation between high and low frequency radio emission has led to the standard assumption that these cavities are filled with relativistic plasma (Bîrzan et al., 2004). However, the short age and steep spectrum of many of these radio sources imply that they may no longer be energizing the cavities. Alternatively, the cavities may be filled with a very hot thermal plasma that is inflating them. The temperature of this plasma would have to be very high (> 20 keV to avoid detection in the *Chandra* bandpass. This scenario would seem to be consistent with the SZE map shown in Figure 1 which clearly shows the signature of very hot $T \sim 25$ keV plasma distributed throughout the core of RXJ1347.5-1145. This result is corroborated by the recent *Suzaku* detection of 25 keV thermal plasma in RXJ1347.5-1145 (Ota et al., 2008). We note in particular that the spatial distribution of the very hot gas implied by the SZE map includes the area corresponding to the possible cavity system discussed here and not just the SE X-ray enhancement which has been previously noted. When combined with the existing SZE and *Suzaku* data, the temperature maps that will result from these observations will place strong limits on the thermal content of the cavities.
- **Constrain Possible Shock Parameters:** The observed sharp surface brightness features noted in Figure 1 may represent the signature of shocks associated with an ongoing merger event. As discussed above, although there are a number of apparent discrepancies with this interpretation, the proposed deep *Chandra* imaging will allow us to measure the density, temperature and pressure of the ICM at $\sim 2''$ resolution over the entire region inside $30''$. Neglecting projection effects, this scale corresponds to the collisional mean free path for Coulomb interactions in the plasma and is therefore a reasonable estimate for the intrinsic width of the shock (Mason et al., 2009). If these features can be confirmed as shocks, we will derive estimates for the ages and energies. Regardless of whether these features are associated with shocks, cold fronts, or cavity rims, the requested observations will provide high quality maps of the physical state of the ICM in the core. These will in turn yield strong constraints on both the magnitude and location of heating (or cooling) in RXJ1347.5-1145.
- **Measure AGN Energetics:** If the cavity structures shown in Figure 1 are indeed linked to an AGN outburst, we can determine the AGN jet power using the by now standard method of measuring the cavity volumes (V) and surrounding pressures (p) to determine the work done by the jet in inflating the cavities. These techniques can yield robust measurements of the total free energy in the cavity system, $E = [\gamma/(\gamma - 1)]pV$, modulo a factor of two uncertainty about the state of the gas filling the cavity. Values can range from $2.5 - 4pV$ depending on whether the cavity is filled with an ideal gas ($\gamma = 5/3$) or relativistic plasma ($\gamma = 4/3$), respectively. Cavity ages can be determined either from sound speed travel time or buoyant rise time arguments and combined with the energy measurements to yield an estimate of the

total AGN output power. The requested deep exposure will allow us to formally constrain the AGN jet output to within a factor of two. These values can then be combined with other energy metrics such as the total implied X-ray cooling rate or energy injection due to a merger event to understand the total energy budget in the core of RXJ1347.5-1145.

- **Black Hole Growth at High Redshift:** For an assumed accretion efficiency, ϵ , the derived values for the AGN jet power can be used to constrain the mean accretion rate on the black hole using $\dot{M} \approx 4pV/t\epsilon c^2$, where values of $\epsilon \approx 0.1$ are typically assumed. These estimates can then be used in turn to estimate the growth of black holes over time. Similar analyses have been performed for samples of cluster cavity systems at lower redshifts (Rafferty et al., 2006). Given the apparent correlation between black hole growth and galaxy assembly (Magorrian et al., 1998), extending these samples to higher redshift is essential. At a redshift of $z = 0.451$, an accurate measurement of the black hole growth rate in RXJ1347.5-1145 would be one of the most distant yet determined.
- **High Quality Mass Profiles:** As the most luminous X-ray cluster known, RXJ1347.5-1145 has been the subject of a number of strong and weak lensing analyses (Miranda et al., 2008; Halkola et al., 2008; Lu et al., 2010). A deep, high resolution X-ray image of the structure in the core will be a valuable addition to future combined strong lensing + X-ray analyses of the mass distribution in RXJ1347.5-1145. Similarly, as a by-product of the proposed observations, we will produce high quality profiles of the X-ray gas mass and total cluster mass out to several Mpc.

4 Complimentary Data on RXJ1347.5-1145

In addition to the archival X-ray data, we have also obtained low frequency radio GMRT observations for this object. The presence of radio emission filling the observed X-ray cavity structures has been one of the key pieces of evidence connecting these structures to activity from the central AGN. Specifically, low frequency radio data have been shown to be an excellent tracer for the integrated energy output required to produce the cavities (Bîrzan et al., 2008). With this correlation in mind, we have recently obtained 6 hr integrations at 215 MHz and 610 MHz with the GMRT. At these frequencies, the GMRT has an effective spatial resolution of 15 arcsec and 5 arcsec, respectively. Although not sufficient to resolve most of the features seen in Figure 1, these data can nonetheless be used to look for larger scale radio morphologies consistent with a AGN outbursts.

These data will also be augmented by higher resolution, low-frequency observations with LOFAR in the Spring of 2011. LOFAR is a new radio telescope under construction in Europe and optimized to work in the 30-240 MHz band. The array is largely complete and currently in a commissioning and verification phase. With baselines from 100 km out to 1000 km, LOFAR will ultimately achieve spatial resolutions of 0.2-2.0 arcsec over this frequency range. RXJ1347.5-1145 will be observed this Spring as part of an initial commissioning survey. Several of the investigators on this proposal are part of the LOFAR project and will have early access to these data as they become available. At these resolutions, the LOFAR images and *Chandra* spectral maps can be examined directly for possible correlations between the putative cavity structures and the observed radio emission.

5 Instrumental Setup and Exposure Time Justification

We propose to obtain a deep exposure of the core of the RXJ1347.5-1145 cluster. Given the high mean temperature of the cluster, the increased sensitivity of the ACIS-S3 below 2.0 keV provides no real advantage so we will use the ACIS-I detector. The lower background in the ACIS-I will

also maximize our sensitivity to faint surface brightness features at larger radii. The larger field of view of ACIS-I will also be useful for accurately determining the surface brightness profile to large radii and as well as the cluster mass inferred from that profile. The VF datamode will be used to improve rejection of background events. To avoid complications associated with the ACIS-I chip gaps, we will offset the cluster center by at least an arcminute from the CCD boundaries.

The majority of the science goals described in Section 3 depend on the ability to map the central arcminute of RXJ1347.5-1145 with reasonably high accuracy both spatially and spectrally. In particular, we wish to define a grid that adequately samples the locations of the possible cavities as well as the sharp surface brightness features possibly related to shocks or cold fronts. Spatially this requirement sets a limit on the necessary cell sizes of between $1'' \times 1''$ and $5'' \times 5''$ within the inner 30 arcsec. Such a requirement would allow 10-15 independent measurement cells on all of the major morphological features including the two possible cavity areas and the area of enhanced temperature in the SE. It would also result in 2-4 independent measurement cells arrayed across the sharp surface brightness features indicated in Figure 1. To achieve a good quality spectrum in each measurement cell, we require a minimum of 2000 counts per cell in the 0.5-7.0 keV band after background subtraction. In the literature, spectral maps are often made with less counts per cell; however, given the high gas temperature in RXJ1347.5-1145 and the dropping *Chandra* sensitivity at these temperatures, a more conservative choice seems appropriate.

Taking these constraints, we can crudely estimate the required exposure time using the existing 63 ksec (after filtering) of RXJ1347.5-1145 data from the *Chandra* archive. Within the inner $30''$ (172 kpc) encompassing the possible cavities, the SE enhancement, and the sharp surface brightness discontinuities, the mean count rate is 7.6×10^{-5} cts s $^{-1}$ pixel $^{-2}$. In order to obtain ~ 2000 counts within an average $4'' \times 4''$ detection cell, we would therefore require an exposure time of ~ 410 ksec. This exposure would consequently result in smaller detection cells of the same spectral quality on and around the higher surface brightness regions in the core.

To refine this estimate, we have performed a series of MARX simulations of RXJ1347.5-1145 using the exposure-corrected image shown in Figure 1 as an input source model. The shape of the source spectrum and overall flux normalization were taken from a fit to the total spectrum inside 100 arcsec (0.6 Mpc). Simulations were run for a number of exposure times and for each simulation the contour binning algorithm of Sanders (2006) was used to calculate the resulting mapping grid given the 2000 counts per cell criterion. Each grid was then visually inspected to determine whether sufficient cells were distributed across the core region. Based on this analysis, we conclude that a total exposure time closer to 500 ksec is optimal. Given the existing 63 ksec of *Chandra* data, we are therefore proposing an additional 440 ksec observation of RXJ1347.5-1145.

6 References

- Allen, S. W., Schmidt, R. W., & Fabian, A. C. 2002, MNRAS, 335, 256
 Birzan, L., McNamara, B. R., Nulsen, P. E. J., Carilli, C. L., & Wise, M. W. 2008, ApJ, 686, 859
 Birzan, L., Rafferty, D. A., McNamara, B. R., Wise, M. W., & Nulsen, P. E. J. 2004, ApJ, 607, 800
 Gitti, M., Ferrari, C., Domainko, W., Feretti, L., & Schindler, S. 2007, A&A, 470, L25
 Gitti, M., & Schindler, S. 2004, A&A, 427, L9
 Halkola, A., Hildebrandt, H., Schrabback, T., Lombardi, M., Bradač, M., Erben, T., Schneider, P., & Wuttke, D. 2008, A&A, 481, 65
 Kitayama, T., Komatsu, E., Ota, N., Kuwabara, T., Suto, Y., Yoshikawa, K., Hattori, M., & Matsuo, H. 2004, PASJ, 56, 17
 Komatsu, E., Matsuo, H., Kitayama, T., Hattori, M., Kawabe, R., Kohno, K., Kuno, N., Schindler, S., Suto, Y., & Yoshikawa, K. 2001, PASJ, 53, 57
 Lu, T., Gilbank, D. G., Balogh, M. L., Milkeraitis, M., Hoekstra, H., van Waerbeke, L., Wake, D. A., Edge, A. C., & Bower, R. G. 2010, MNRAS, 184
 Magorrian, J., Tremaine, S., Richstone, D., Bender, R., Bower, G., Dressler, A., Faber, S. M., Gebhardt, K., Green, R., Grillmair, C., Kormendy, J., & Lauer, T. 1998, AJ, 115, 2285
 Mason, B. S., Dicker, S. R., Korngut, P. M., Devlin, M. J., Cotton, W. D., Koch, P. M., Molnar, S. M., Sievers, J. L., Aguirre, J. E., Benford, D., Staguhn, J. G., Moseley, H., Irwin, K. D., & Ade, P. A. R. 2009, ArXiv e-prints
 Miranda, M., Sereno, M., de Filippis, E., & Paolillo, M. 2008, MNRAS, 385, 511
 Ota, N., Murase, K., Kitayama, T., Komatsu, E., Hattori, M., Matsuo, H., Oshima, T., Suto, Y., & Yoshikawa, K. 2008, A&A, 491, 363
 Pointecouteau, E., Giard, M., Benoit, A., Désert, F. X., Aghanim, N., Coron, N., Lamarre, J. M., & Delabrouille, J. 1999, ApJ, 519, L115
 Pointecouteau, E., Giard, M., Benoit, A., Désert, F. X., Bernard, J. P., Coron, N., & Lamarre, J. M. 2001, ApJ, 552, 42
 Rafferty, D. A., McNamara, B. R., Nulsen, P. E. J., & Wise, M. W. 2006, ApJ, 652, 216
 Sanders, J. S. 2006, MNRAS, 371, 829
 Schindler, S., Hattori, M., Neumann, D. M., & Boehringer, H. 1997, A&A, 317, 646